Freezing conditions in warm disks: snowlines and their effect on the chemical structure of planet-forming disks

Leemker, M.

Chapter 3

Resolving snow surfaces of water and methanol in the V883 Ori disk

M. Leemker, T. Paneque-Carreño, J. J. Tobin, M. L. R. van 't Hoff, E. F. van Dishoeck, and A. S. Booth

In preparation

Abstract

Context. The chemical composition of the planet forming material changes around the major snowlines, those of water and CO, in a protoplanetary disk. The location and shape of the vertical snow surfaces of different molecules can be used to trace vertical mixing in disks and the structure of ices.
Aims. We aim to locate the snow surface of HDO and methanol in the V883 Ori disk in both the radial and vertical direction.
Methods. The ALFAHOR package is used to analyze the emitting height of HDO and methanol in the V883 Ori disk observed with ALMA.
Results. We find that the HDO and methanol snow surfaces are close to vertical, consistent with the vertical cold finger effect that transports water to the disk midplane due to diffucion and vertical mixing of grains. The HDO emission is seen in the midplane out to ~ 60 au pointing to a water snowline location beyond 60 au. Additionally, the methanol snow surface is located $\sim 10 - 20$ au outside that of HDO consistent with the lower binding energy of methanol to the grains. The separation between the two snow surfaces indicates that methanol is not co-desorbing with water ice.
Conclusions. The HDO and methanol snow surfaces in the V883 Ori disk are steep and radially separated indicating that methanol does not co-desorb with water. Therefore, the V883 Ori disk provides a unique laboratory to observationally determine the binding energies of other complex organic molecules.

3.1 Introduction

The thermal structure of protoplanetary disks has a large effect on the outcome of planet formation. In particular, snowlines, the midplane radii where 50% of a molecule is frozen out as ice and 50% is in the gas-phase, are important as they mark special locations in the disk where the chemical composition of the planet forming gas and ice changes due to selective freeze-out (see Öberg & Bergin 2021, for a recent review). In addition, the increase in the surface density of solids just outside the water snowline can aid planet formation by triggering the streaming instability leading to grain growth (e.g., Stevenson & Lunine 1988; Drążkowska & Alibert 2017; Pinilla et al. 2017).

Vertically the snowline is thought to follow the line where the freeze-out and desorption rates balance. This snow surface thus follows the temperature structure of the disk, and to some degree also its density structure, with the snow surface moving up as the radius increase. Recently, Bosman & Bergin (2021) proposed that the water snow surface may instead be vertical due to the continuous vertical mixing of grains in disks, following the idea of a vertical cold finger effect (Meijerink et al. 2009). In this scenario grains are mixed up to high layers in the disk where gas-phase water is abundant. Then water freezes-out and the grains settle to the disk midplane where these grains grow and become too heavy to be efficiently mixed up again. This causes a vertical water snow surface in disks and a similar process is expected for other molecules that freeze-out in disks such as CO and complex organic molecules (COMs).

COMs are suggested to desorb sequentially due to the different binding energies on the grains for different COMs. For example, observations of young and massive protostars show warm formamide at $300-400$ K, whereas an isotopologue of methanol $CH_3^{18}OH$ is seen at only 100 K (e.g., Jørgensen et al. 2018; Nazari et al. 2022). As the temperature profile of protostellar envelopes decreases with increasing distance to the star, the $CH_3^{18}OH$ traces colder and thus more extended material than the warmer formamide. Similarly, differences are expected for other COMs such as acetaldehyde (CH_3CHO) that has a lower binding energy than e.g., methanol (Penteado et al. 2017; Minissale et al. 2022) and its snow surface is thus expected to be further away from the central star. However, the binding energy of a molecule depends on the surface to which it is bound. Therefore, acetaldehyde ice that is frozen on top of a methanol ice layer may have a different sublimation temperature than if it is frozen out onto a water ice layer.

The ice on grains in disks likely consists of multiple layers with different molecules in each layer. This is due to the formation of ices in the parent molecular cloud and the formation of molecules on the icy surfaces. For example, laboratory research shows that some COMs like acetaldehyde and ethanol formed in a layer with both water and C_2H_2 ice, may be trapped in the water ice matrix whereas COMs that form through CO hydrogenation e.g., CH_2OHCHO, $(CH_2OH)_2$, and CH_3OCHO may be trapped in methanol ice that is also formed through CO hydrogenation (Chuang et al. 2020; Simons et al. 2020). Two molecules that may also have a common formation pathway are NH_2CHO and HCNO as they have a very similar spatial distribution in the HH 212 protostellar disk system (Lee et al.

2022). Therefore, information on the order in which molecules desorb in a protostellar envelope and at which disk locations can shed light on the ice structure and thus the formation pathways of COMs and other molecules on the grains.

The midplane location where water and CO desorb have been located using chemical tracers such as HCO^+ (for water) and N_2H^+, DCO^+, and very rare CO isotopologues (for CO) (van 't Hoff et al. 2017; Carney et al. 2018; van 't Hoff et al. 2018a; Qi et al. 2019; Leemker et al. 2021). A second method to derive the water snowline location is to use the emission of COMs that desorb at approximately the same temperature as water (van 't Hoff et al. 2018b; Booth et al. 2023c). However, these methods only work for molecules like water and CO for which tracers are available. Observations of embedded edge-on disks show the 2D snow surface of each molecule that is observed as the column density in the disk midplane and beyond will be greatly reduced due to freeze-out (e.g., Podio et al. 2020; van't Hoff et al. 2020; Lee et al. 2022). Yet, models by Sturm et al. (2023c) show that the situation is much more complicated in Class II disks at infrared wavelengths.

Recently, a new method has become available to study the emitting surfaces in moderately inclined protoplanetary disks using the Keplerian rotation that can be seen in high spatial and spectral resolution channel maps (Pinte et al. 2018a). This work presented the emitting surfaces of ^{12}CO, ^{13}CO, and C^{18}O in the IM Lup disk and found that the latter two are co-located at roughly 20 K. This is a direct indication that the emitting surfaces trace snow surfaces if the emission is not highly optically thick. In addition, analyses of many different molecules across the disks shows that the molecules span a wide range of vertical emitting heights depending on the optical depth (e.g., for CO isotopologues), upper energy level of the transition (e.g., ^{13}CO $J = 2 - 1$ vs $J = 6 - 5$), and the abundance structure (e.g, for CN) (Law et al. 2021b; Leemker et al. 2022; Paneque-Carreño et al. 2022, 2023; Law et al. 2023b).

In this work we focus on the V883 Ori disk. This disk is located around an outbursting star with a luminosity of ~ 200 $L_\odot$ that has heated the disk and shifted the water snowline out to at least 40 au but possibly as far as 120 au (Cieza et al. 2016; Furlan et al. 2016; van 't Hoff et al. 2018b; Leemker et al. 2021). The disk is located in Orion at ~ 400 pc (Kounkel et al. 2017) and has a moderate inclination of 38° (Cieza et al. 2016). This disk is the most COM rich disk to date (Lee et al. 2019). Additionally, other molecules such as the potential precursor of methanol, and both HDO and methanol have been observed at high spatial and spectral resolution and sensitivity in this disk (Ruíz-Rodríguez et al. 2022; Tobin et al. 2023). In addition to the circumstellar disk, the system is surrounded by a remnant envelope (e.g., Ruíz-Rodríguez et al. 2017).

This paper is organised as follows. In Sect. 3.2 we outline the method used to derived the emitting surfaces of HDO and methanol in the V883 Ori disk. The results are presented in Sect. 3.3 and in Sect. 3.4 the implications for the structure of the ice on the dust in protoplanetary disks are discussed and compared to other sources. Finally, our conclusions are summarised in Sect. 3.5.

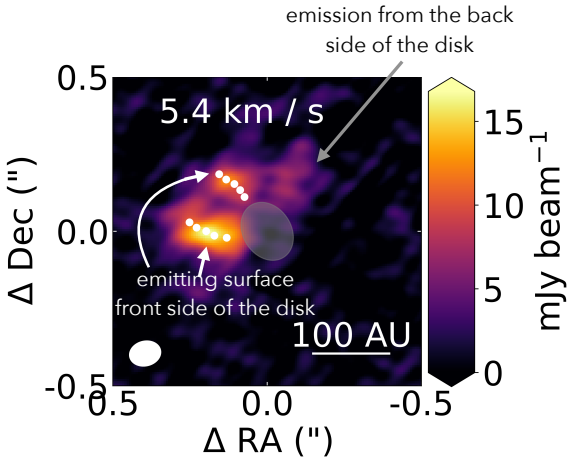

Figure 3.1: Channel map of the HDO 225 GHz emission at 5.4 km s^{-1} which is 1.3 km s^{-1} from the source velocity of 4.3 km s^{-1} (van 't Hoff et al. 2018b). The white dots indicate the emission peaks of the near and far side of the disk's front side. The grey arrow indicates the emission from the near and back side of the disk. The grey ellipse in the center indicates a 40 au radius within which the continuum emission is optically thick and the HDO emitting surface cannot be traced.

3.2 Methods

To derive the emitting heights, observations with a high signal-to-noise ratio taken at a high spatial ($\lesssim 0\farcs15$) and a high spectral resolution ($\lesssim$ 0.2 km s^{-1}) of unblended lines. Most archival ALMA data sets do not satisitfy at least one of these criteria. Therefore, we focus here on the HDO and methanol presented in Tobin et al. (2023, ALMA project code: 2021.1.00186.S). In particular, the HDO 225 GHz line is used as the 241 GHz line is heavily blended confusing the HDO and COM emission in the channel maps. For methanol we used the stacked channel maps of the six isolated methanol lines to increase the signal-to-noise ratio, see Table 3.1. Both lines were imaged at a spatial resolution of $0\farcs10 \times 0\farcs08(-76.6°)$ and $0\farcs09 \times 0\farcs07(-75.2°)$ for HDO and methanol, respectively, and a spectral resolution of 0.16 km s^{-1}. Details about the imaging of the data can be found in Tobin et al. (2023).

The emitting height of the HDO and methanol emission is inferred directly from the channel maps using the ALFAHOR package (Paneque-Carreño et al. 2023), based on Pinte et al. (2018a). Masks encompassing the upper emitting surface in the near and far side of the disk were created after visual inspection of the data to exclude emission from the lower disk surface and from neighbouring COMs. Subsequently, the emission maxima along the major axis are located within these masks in the near and far side of the disk by the ALFAHOR package. Fig. 3.1 shows the resulting peak locations for the HDO channel at 5.4 km s^{-1}, whereas the source velocity is 4.3 km s^{-1} (van 't Hoff et al. 2018b). The channel maps of the

Table 3.1: HDO and methanol lines used in this work.

Molecule	Frequency (GHz)	Transition	$\log_{10} A_{ij}$ (s^{-1})	E_{up} (K)
HDO	225.897	$3(1,2) - 2(2,1)$	-4.9	168
CH_3OH	241.807	$5(4)^- - 4(4)^-$ $v_t = 0$	-4.7	115
CH_3OH	241.807	$5(4)^- - 4(4)^-$ $v_t = 0$	-4.7	115
CH_3OH	241.813	$5(-4) - 4(-4)$ E_2 $v_t = 0$	-4.7	123
CH_3OH	241.852	$5(-3) - 4(-3)$ E_2 $v_t = 0$	-4.4	98
CH_3OH	241.879	$5(1) - 4(1)$ E_1 $v_t = 0$	-4.2	56
CH_3OH	241.888	$5(2)^+ - 4(2)^+$ $v_t = 0$	-4.3	73

The line properties are obtained from the JPL database (Johns 1985; Pickett et al. 1998; Xu et al. 2008).

methanol and HDO emission with the masks and traced maxima are presented in Fig. 3.A.1 and 3.A.2. For each pair of points the spatial location of the maxima is converted to an emitting height using an position angle of 32.4°, an inclination of 38.3° and a distance of 400 pc. A linear fit was made to the resulting data points that lie above the midplane and inside 80 au. Furthermore, the emitting heights are binned to increase the signal-to-noise ratio.

3.3 Results

The resulting emitting heights of the HDO and methanol emission are presented in Fig. 3.2. The scatter points in this figure indicate the emitting height derived from each pair of a near and a far side emission peak. To increase the signal-to-noise ratio, these data points are binned resulting in the thick blue line with the shaded region indicating the scatter. The emitting surfaces are only traced outside 40 au where the dust is not highly optically thick at mm-wavelengths (Cieza et al. 2016). Outside this region, the emitting surfaces trace the snow surfaces of HDO and methanol, respectively, as these molecules are expected to be frozen out in the disk midplane. If the emission is optically thin or marginally optically thick, the traced surface is set by the region with the highest density of HDO or methanol molecules. As the gas density increases towards the disk midplane and the HDO and methanol emission is marginally optically thick (see Appendix 3.B for details), the highest HDO and methanol densities are found just above their respective snow surfaces.

Gas-phase water is seen close to the disk midplane out to $\sim$ 60 au. This is close to consistent with the $75 - 120$ au midplane snowline location derived from previously observed methanol and HCO^+ emission (van 't Hoff et al. 2018b; Leemker et al. 2021), whereas this is 20 au further out than sudden change in the continuum opacity at 40 au attributed to the water snowline (Cieza et al. 2016).

The resulting emitting surface of both HDO and methanol are very steep, rising $\gtrsim$ 30 au in height over a radial region of 20 au. This is much steeper and more

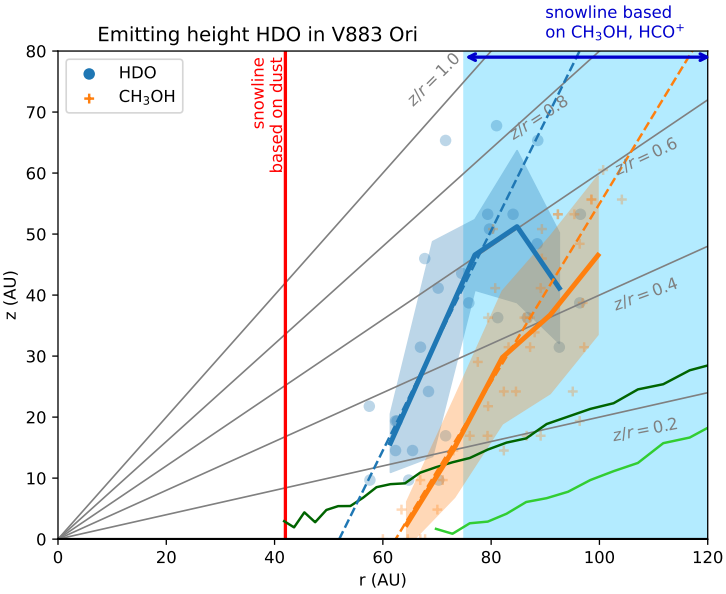

Figure 3.2: Emitting surface of the HDO 225 GHz and methanol emission in the V883 Ori disk. The scatter points indicate the measured height and the thick blue and orange lines the binned surface of HDO and methanol, respectively. The dashed lines indicate a linear fit to the points inside 80 au. The vertical red line indicates the ~ 40 au midplane water snowline location based on the continuum (Cieza et al. 2016) and the blue shaded region indicates the midplane water snowline based on previously detected methanol and HCO^+ emission (van 't Hoff et al. 2018b; Leemker et al. 2021). Finally, the dark and light green lines indicate the water snow surfaces for the V883 Ori disk radiative transfer models with a snowline at 47 au and 76 au presented in Leemker et al. (2021).

vertically extended than expected based on the temperature of thermochemical models (green lines in Fig. 3.2, Leemker et al. 2021). This is likely not due to molecular excitation as the HDO line at 225 GHz has an upper energy level of 167 K, similar to the desorption temperature of H_2O (Penteado et al. 2017). Therefore, even if the measured emitting surface would mainly trace gas at this temperature, this would still coincide with the water snow surface. Moreover, the stacked methanol lines cover a range of different upper energy levels ($56 - 123$ K) and still trace similar disk regions.

The emitting surfaces above the disk midplane and inside 80 au follow an approximately linear relation. Outside 80 au the scatter increases and the emitting heights cannot be traced accurately. A linear fit to the surfaces inside 80 au and above the midplane shows that the slope of both surfaces are similar with an increase of 1.8 au and 1.5 au in height for every au in radius for HDO and methanol, respectively. Extrapolating this to the disk midplane shows that the last radius where gas-phase HDO and methanol are present is 52 au and 62 au,

respectively.

The radial off-set between HDO and methanol persists above the disk midplane with the emitting surface of methanol being shifted to larger radii by $\sim 10-20$ au than that of HDO. Such an off-set is expected as the binding energy of H_2O of 5770 K is higher than that of methanol of 3800 K (Penteado et al. 2017). Therefore, H_2O is expected to desorb at a higher temperature and thus closer to the central star than methanol. The clear separation between the measured emitting surfaces also indicates that most of the methanol ice desorbs at its own desorption temperature rather than being locked up in a water ice matrix.

3.4 Discussion

The distinct difference between the location of the HDO and methanol snow surfaces indicates a true difference in the abundance structure of the two molecules in the disk or a difference in the excitation of the two molecules. The HDO emitting surface is traced using a 167 K line whereas the methanol surface is traced using a stacked image of six methanol lines with upper energy levels ranging from 56 to 123 K. Observations of CO isotopologue emission in other protoplanetary disks around T Tauri and Herbig stars show that transitions with low upper energy levels generally emit from lower disk layers as the disk temperature decreases towards the disk midplane (Leemker et al. 2022; Paneque-Carreño et al. 2023). This could contribute to the observed difference in the emitting surfaces of HDO and methanol. However, the methanol surface is derived from a stacked image of six transitions to increase the signal-to-noise ratio. A low signal-to-noise analysis of the individual transitions did not reveal large differences between the emitting layers of lines with high ($\sim$ 123 K) and low ($\sim$ 56 K) upper energy levels. Therefore, excitation may contribute but is not expected to the the dominant driver of the radial offset between HDO and methanol. Thus, a difference in the underlying abundance structure due to the snow surface of HDO and methanol is likely responsible for the different emitting surfaces.

3.4.1 Layered or mixed ices on the grains

A difference in the underlying abundance structure could be caused by a difference in the sublimation temperature of HDO and methanol. Modelling of ice layers on grains shows that water and methanol are expected to be abundant in different layers as water is formed the hydrogenation of O and methanol through hydrogenation of CO ice (Taquet et al. 2012). Laboratory studies show that methanol sublimates at a temperature 20 K lower than water if the methanol ice is deposited on top of the water ice matrix (Collings et al. 2004). On the other hand, if the ices are mixed, methanol and water sublimate at the same temperature. However, other laboratory experiments show that for a pre-cometary ice mixture (H_2O:CH_3OH:CO:CO_2:NH_3=100:5.7:8.7:20.2:5.7), the methanol desorbs in multiple stages including desorption at the temperature of a pure ice matrix and co-desorption with water (Martín-Doménech et al. 2014). Co-desorption of methanol

with the much more volatile CO ice has not been seen in experiments (Ligterink et al. 2018b). Therefore, the radial offset between the HDO and methanol snow surfaces in the V883 Ori disk could point to a layered ice structure instead of a mixed one. Wether this also holds for other molecules requires high spatial and spectral resolution observations of multiple molecules at high sensitivity.

In addition to the structure of the ices (segregated layers or mixed), the amount of ice on the grains also affects the sublimation temperature, as only the top layer of ice can sublimate efficiently. Zeroth order sublimation is the process for a thick ice layer consisting of multiple mono-layers. This ice desorbs at a temperature depending on the concentration with an increasing temperature for thicker ices. First order sublimation is relevant for ices that cover less than one mono-layer on the surface. Because this is the top layer, the desorption temperature is independent of the fractional coverage of the grain surface. As the ice on grains in protoplanetary disks is dominated by water ice, the desorption of water may follow a zeroth order profile, whereas the less abundant methanol ice could be dominated by a first order process. In particular, Minissale et al. (2022) find that in this case a monolayer of methanol ice on an amorphous water ice layer desorbs at a somewhat lower temperature than water in the laboratory, consistent with the results in the V883 Ori disk. Observations of $^{13}CH_3OH$ and $H_2^{18}O$ in the V883 Ori disk show that the water to methanol ratio is 6 after correcting for the isotopologue ratios but not correcting for the optical depth of the dust (Lee et al. 2019; Tobin et al. 2023). Therefore, the difference between zeroth and first order desorption could contribute to the difference in the HDO and methanol snow surfaces that are observed. However, the abundance of HDO is much lower than that of H_2O so both HDO and methanol are much less abundant than H_2O in the ice. In addition, methanol ice generally extends multiple monolayers. Therefore, the effect of zeroth and first order desorption may contribute somewhat to the difference in the emitting surfaces, but it is not expected to be the dominant driver.

3.4.2 HDO and methanol snow surfaces in other disks

HDO and methanol have both been observed in the edge-on protostellar disk around the HH 212 system. The emitting region of methanol is constrained to a ~ 15 au thick layer that is elevated above the disk midplane at radii larger than 19 au up to a radius of ~ 40 au where the layer extends from $15-30$ au (Lee et al. 2022). Therefore, the largest midplane radius where gas-phase methanol is seen in this disk is 19 au. Additionally, the emitting region of HDO in the same disk is constrained to be < 60 au using a warm transition (Codella et al. 2018). As the < 60 au radius of the water emitting region in this disk is potentially much larger than that of methanol, the upper limit is not sufficiently stringent to determine the order of the snowlines in the HH 212 disk, though the results could be consistent with those found in the V883 Ori disk presented in this work.

The snow surface of other molecules such as CO, CS, and H_2CO have been spatially resolved in the edge-on disks L1527 IRS and IRAS 04302+2247 (van't Hoff et al. 2020; Podio et al. 2020). Additionally, a tentative detection of methanol in the L1527 IRS disk has been reported, though similar observations did not detect

methanol in the same disk. The emitting surfaces of CO, CS, and H_2CO in these edge-on disks are much more shallow with a slope $\Delta z/\Delta r \lesssim 1$ than those seen in the V883 Ori disk. This could be due to a difference in the evolutionary stage of the objects as the V883 Ori disk is located around an outbursting Class I/II star whereas the L1527 IRS and IRAS 04302+2247 disks are not and are still embedded. Additionally, the difference in the slope of the snow surfaces could be due to a difference in vertical mixing between the disks. Bosman & Bergin (2021) suggested that the water snowline in the AS 205 disk may be vertical due to continuous vertical mixing, locking the water as ice in the disk midplane. If this mechanism is the dominant mechanism driving the slope of the snowline in these three disks, then the vertical mixing may be more efficient in the V883 Ori disk than in the L1527 IRS and IRAS 04302+224 disks.

3.5 Conclusions

In this work we present the emitting surfaces of HDO and methanol, the only two molecules observed at sufficiently high spatial and spectral resolution and sensitivity that are not dominated by the remnant envelope emission to derive the emitting heights. The emitting surfaces are measured using the ALFAHOR package (Paneque-Carreño et al. 2023) and provide the first direct measurement of the HDO and methanol snow surfaces in a moderately inclined disk, V883 Ori. In summary we find that:

1. The snow surfaces of HDO and methanol are directly traced by the emitting surface and are close to vertical.
2. Gas-phase HDO is seen in the disk midplane up to ~ 60 au, consistent with a water snowline location > 60 au.
3. The emitting surface of methanol is consistently at a $\sim 10 - 20$ au larger radius than that of HDO indicating a difference in their desorption temperatures likely due to a layered ice structure.

The steep snow surfaces seen in the V883 Ori disk could hint at efficient vertical mixing in protoplanetary disks. Observations of other COMs together with optically thin CO isotopologue emission at high spatial and spectral resolution and sensitivity are needed to derive their snow surfaces and the structure of the disk as traced by CO isotopologues. This will provide insights in the ices present on the grains together with crucial information to interpret unresolved observations of e.g. protostellar envelopes. The V883 Ori disk is a unique laboratory to observationally determine the (relative) binding energies of COMs.

3.6 Acknowledgements

We would like to thank Niels Ligterink for useful discussions. This work is supported by grant 618.000.001 from the Dutch Research Council (NWO). Astrochemistry in Leiden is supported by funding from the European Research Council

(ERC) under the European Union's Horizon 2020 research and innovation programme (grant agreement No. 101019751 MOLDISK), by the Netherlands Research School for Astronomy (NOVA). This paper makes use of the following ALMA data: ADS/JAO. ALMA#2021.1.00186.S. ALMA is a partnership of ESO (representing its member states), National Science Federation (NSF) (USA) and NINS (Japan), together with NRC (Canada), MOST and ASIAA (Taiwan), and KASI (Republic of Korea), in cooperation with the Republic of Chile. The Joint ALMA Observatory is operated by ESO, AUI/NRAO and NAOJ. The National Radio Astronomy Observatory is a facility of the National Science Foundation operated under cooperative agreement by Associated Universities, Inc.

Appendix

3.A Channel maps

In this section the channel maps of the HDO and the stacked methanol lines are presented, see Fig. 3.A.1 and 3.A.2. The blue and white contours indicate the masks drawn after visual inspection of the emission in the near and far side of the disk respectively.

3.B Optical depth

The optical depths of the HDO and methanol lines is estimated using RADEX (Schöier et al. 2005). The typical peak intensity of the 225 GHz HDO line is 20 mJy beam^{-1} with a maximum of $\sim$ 25 mJy beam^{-1}. Using a line width of 2 km s^{-1} following Lee et al. (2019), and excitation temperature of 200 K following Tobin et al. (2023), and assuming local thermodynamic equilibrium, we find that the typical line optical depth in the disk is 0.3 with a maximum of 0.4. The six stacked methanol lines all have similar Einstein-A coefficients of $(2-6)\times10^{-5}$ s^{-1}. Therefore, only the warmest (123 K) and coldest (56 K) methanol lines used in the stacking are considered. The resulting optical depths for the methanol lines are typically 0.4 (56 K line) and 0.3 (123 K line) with a maximum of 0.4 for both lines. As the other methanol lines have similar Einstein-A coefficients, identical upper state degeneracies, and upper energy levels that fall within the explored range, their optical depth is expected to fall in the same range as well. The stacked methanol image is thus composed of six unblended lines that are marginally optically thick. However, the similar intensity of the six lines may indicate that the emission on the other hand is more optically thick than suggested by this simple calculation. Therefore, the HDO line and probably also the methanol lines with the highest (123 K) and lowest (56 K) upper energy levels are likely marginally optically thick and thus trace the snow surface.

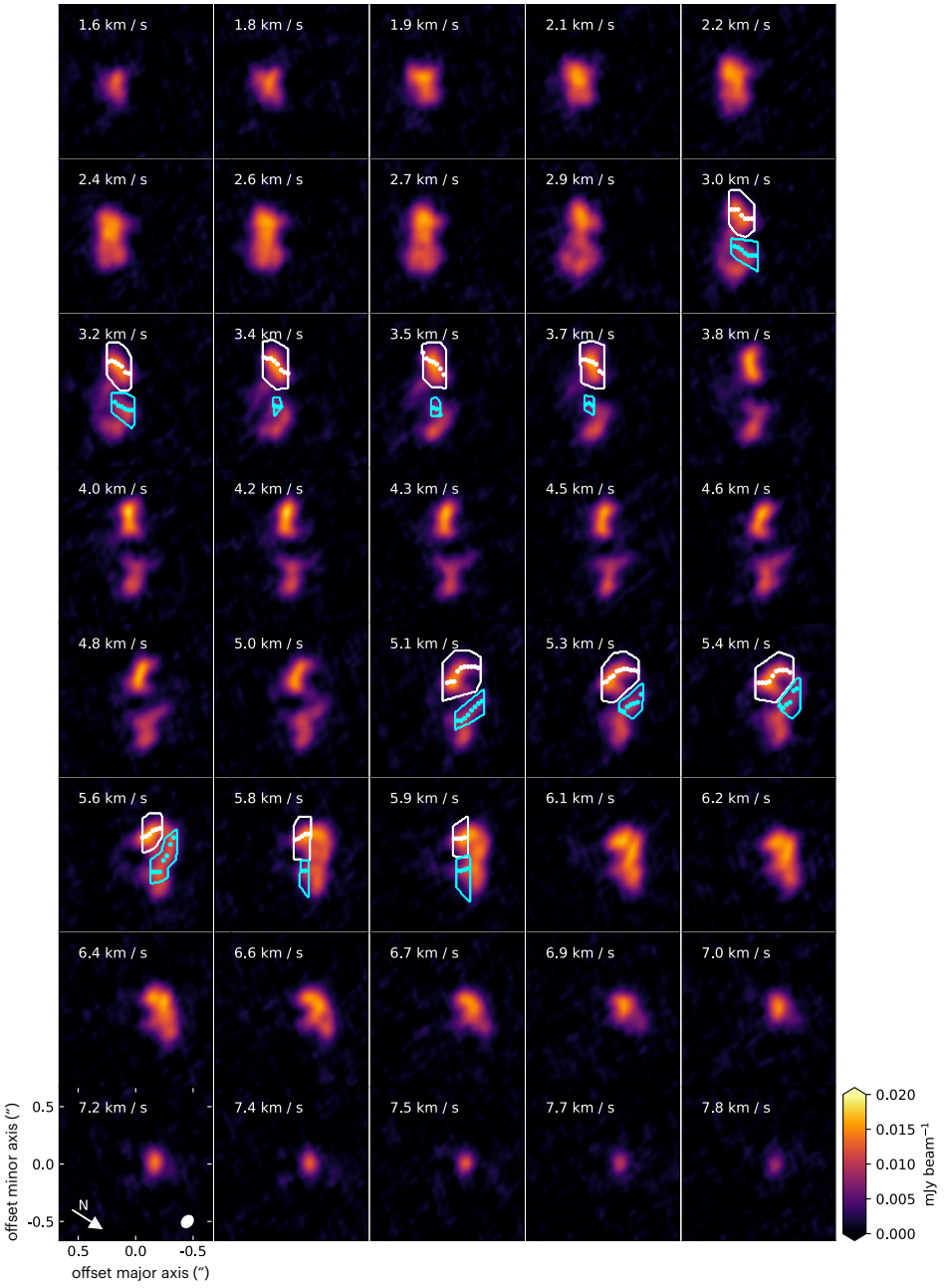

Figure 3.A.1: Channel maps of the stacked methanol emission in the V883 Ori disk. The channel maps are rotated such that the disk major axis is horizontal. North and the beam of the observations are indicated in the bottom left panel by the white arrow and the white ellipse, respectively. The blue (white) contours indicate the masks encompassing the emission from the near (far) side of the disk after visual inspection. The blue (white) dots within the mask trace the emission peak in the direction of the disk major axis.

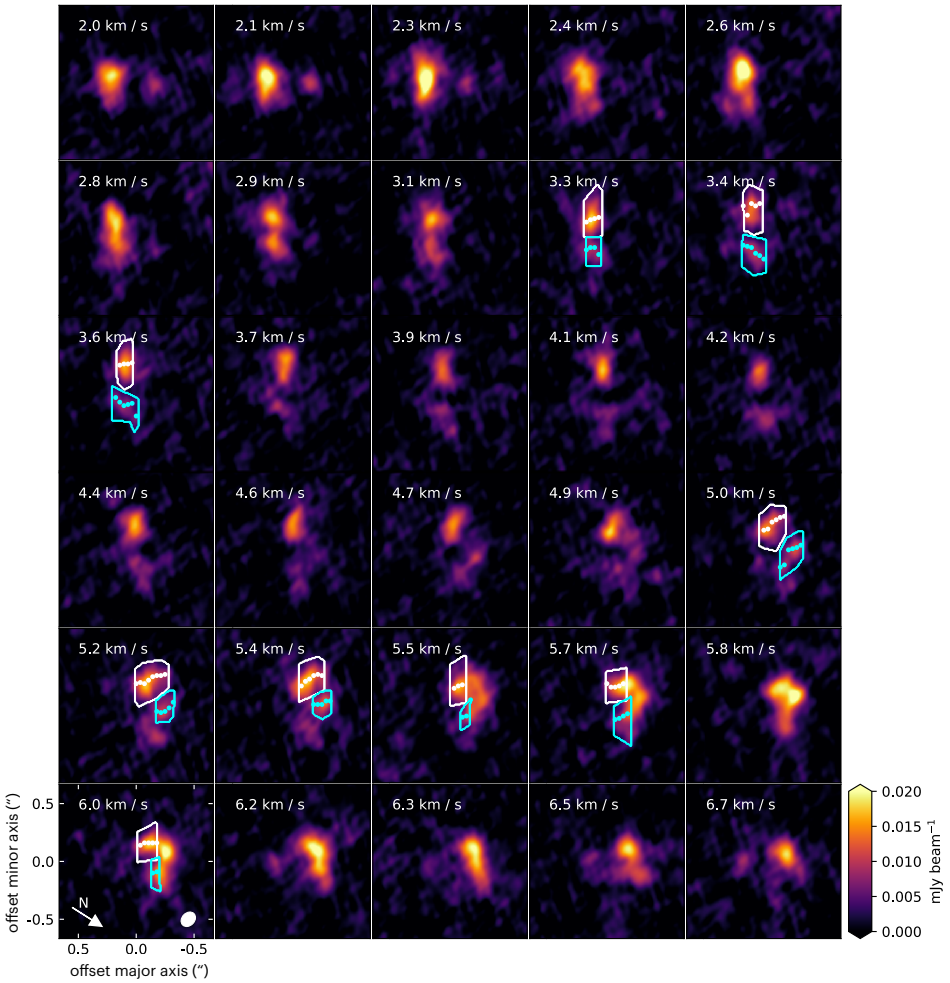

Figure 3.A.2: Same as Fig. 3.A.1 but then for the HDO line at 225 GHz.